

Extended Range of Stable Radial Position of Tokamak Plasma in TOKASTAR-2

Kenji MURAOKA^{a)}, Takaaki FUJITA, Hideki ARIMOTO, Atsushi OKAMOTO, Hiromasa ITOU, Ryoichi SUGIOKA, Masato MINOURA, Kouhei YASUDA, Ryoma YOKOYAMA and Takahiro YAMAUCHI

*Graduate School of Engineering, Nagoya University,
Furo-cho, Chikusa-ku, Nagoya 464-8603, Japan*

(Received 7 January 2018 / Accepted 10 July 2018)

In TOKASTAR-2, the tokamak plasma position was radially unstable in the outer region due to a large decay index (n -index) of the vertical field. To improve the radial position stability, the position of pulsed vertical field coils was moved toward the midplane. After the modification, improvement in the decay index profile and extension of the range of the stable radial plasma position toward the outer region were observed by the internal magnetic field measurement. The variation in the outermost position of the plasma center was about half of the radial shift of the decay index curve.

© 2018 The Japan Society of Plasma Science and Nuclear Fusion Research

Keywords: TOKASTAR, magnetic probe, decay index, plasma position, radial position stability

DOI: 10.1585/pfr.13.1402111

1. Introduction

TOKASTAR-2 is a device confining plasma with the tokamak configuration, the helical configuration and the tokamak-helical hybrid configuration [1–3]. One of the main purposes of the device is to study effects of helical field application on tokamak plasma, where improvement of plasma position stability and suppression of plasma disruption are expected [4–6]. TOKASTAR-2 is a low aspect ratio ($A < 3$) small device with a typical plasma major radius of 0.12 m.

Suppression of oscillation in the horizontal plasma position and improvement of initial rise of the plasma current were observed as effects of the helical field application in TOKASTAR-2 before [7, 8]. However, the helical field application hardly affects dependence of the peak plasma current on the vertical field, which suggests small effects of the helical field on the equilibrium radial plasma position, which was observed in [4]. One possible reason is that the available helical field in TOKASTAR-2, which is limited by the capability of the power supply at present, is not sufficient. The helical field is stronger in the outer region because the modular-type helical coils of TOKASTAR-2 are located outside and on the upper and lower sides of the plasma but not inside. Hence maintaining the plasma in the outer region is favorable for study on the effects of helical field application, but the possible range of the radial plasma position seems to be limited by the radial position instability in TOKASTAR-2.

The plasma position stability is determined by the de-

decay index (n -index) of the vertical field. The decay index is defined by $n = -(R/B_Z^{\text{vac}})(\partial B_Z^{\text{vac}}/\partial R)$ where B_Z^{vac} is the vacuum vertical field and R is the major radius. The vertical position is unstable for n less than 0, while the horizontal position is unstable for n larger than 1.5 [9]. The tokamak plasma position was horizontally unstable in the outer region due to the large decay index in TOKASTAR-2. In order to apply a stronger helical field to the tokamak plasma, the position of the vertical field coils was modified to improve the decay index in the outer region. This paper is organized as follows. Section 2 describes tokamak operation, magnetic field measurement for evaluating the decay index and the radial plasma position, and improvement of the decay index. In Sec. 3, the results of tokamak plasma operation after the modification of the vertical coils are presented. Section 4 describes conclusion.

2. Experimental Setup

2.1 TOKASTAR-2 device and its operation

TOKASTAR-2 coils consist of the tokamak operation coil system and the helical operation coil system, as shown in Fig. 1. In tokamak operation, eight toroidal field (TF) coils generating the toroidal field, ohmic heating (OH) coils inducing the plasma current and a pair of pulsed vertical field (PVF) coils generating the vertical field are used. These three sets of coils are connected to capacitor banks with different capacitance (0.4 mF for the OH coil and 0.2 mF for the TF and the PVF coils) to have the appropriate pulse length for each coil current [3]. No feedback control is available for these circuits and then the current waveforms are determined by the charging voltage of cor-

author's e-mail: fujita@energy.nagoya-u.ac.jp

^{a)} The current affiliation is The Kansai Electric Power Company.

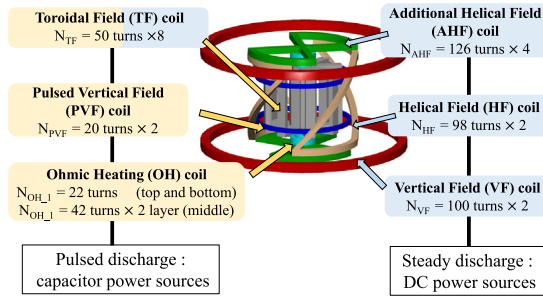


Fig. 1 Coil system of TOKASTAR-2. Yellow text boxes denote coils of the tokamak coil system, and blue text boxes denote coils of the helical coil system. The TF coil is used both for tokamak configuration and helical configuration.

responding capacitor banks. Tokamak plasma is generated inside the poloidal cross-section bounded by the TF coils; $65 \text{ mm} \leq R \leq 180 \text{ mm}$, $-130 \text{ mm} \leq Z \leq 130 \text{ mm}$. In April 2016, a poloidal limiter made of stainless steel was installed to avoid direct contact of plasma to the organic materials on surfaces of TF coils and of the Rogowski coil. The poloidal limiter defines the plasma region of $75 \text{ mm} \leq R \leq 172 \text{ mm}$ and $-120 \text{ mm} \leq Z \leq 120 \text{ mm}$. In parallel with installation of the poloidal limiter, a new poloidal field coil named SC coil was installed and the position of the PVF coils was changed. The SC coil is not used in this study while the modification of the PVF coils is discussed in Sec. 2.3 below.

A typical time sequence of tokamak operation is shown in Fig. 2. At first, the TF coil current starts to rise at $t = 0.45 \text{ ms}$. The toroidal field is 0.11 T at $R = 0.12 \text{ m}$ when the TF coil current reaches the maximum, 160 A , at $t = 2.80 \text{ ms}$. Also at $t = 0.45 \text{ ms}$, 2.45 GHz , 1.4 kW microwave is injected into the vacuum vessel to generate the pre-ionization plasma by electron cyclotron resonance heating (ECRH). The microwave injection is continued until the end of tokamak pulse in usual. In this study, we used nitrogen as the working gas. The pre-ionization plasma is generated at $t = 1.3 \text{ ms}$ when the ECR layer appears on the inner surface of the TF coils. The OH coil current starts to rise at $t = 2.55 \text{ ms}$ and the plasma current is driven. At the same time, the PVF coil current starts to rise and the vertical field is generated to achieve tokamak equilibrium. The peak plasma current is typically $I_p \sim 2.0 \text{ kA}$ and the plasma current is maintained until $t = 3.0 \text{ ms}$.

In the tokamak operation with helical field, the HF coil, the AHF coil and the VF coil are used in addition to the TF, OH and PVF coils. In this paper, the ‘helical field’ denotes the three dimensional vacuum field generated by these three coils. Adding the toroidal field to this ‘helical field’, we can obtain finite rotational transform without the plasma current. The current for the HF, AHF and VF coils are steadily driven during a period including the tokamak pulse. So we cannot turn on the helical field during the tokamak operation but compare the tokamak dis-

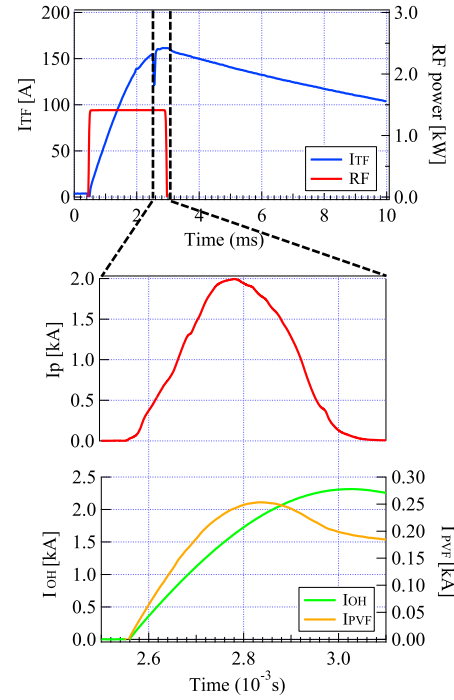


Fig. 2 Typical time sequence of the tokamak operation. The TF coil current I_{TF} and the microwave power (top), the plasma current I_p (middle), and the OH and PVF coil currents, I_{OH} and I_{PVF} (bottom) are shown.

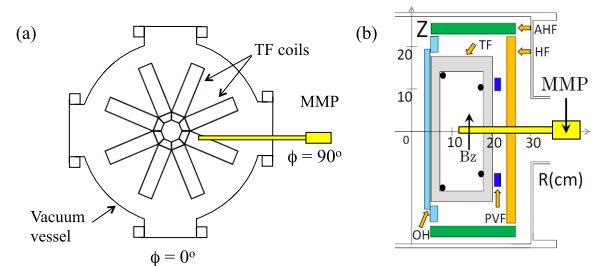


Fig. 3 (a) Plane view and (b) cross section view of TOKASTAR-2.

charges with and without the helical field to investigate the effects of the helical field.

2.2 Magnetic field measurement

The radial distribution of the Z-component of the magnetic field was measured with a new multi-channel magnetic probe, MMP, inserted on the midplane, $Z = 0$. The new MMP was manufactured to improve the sensitivity of the old MMP used before in [7]. The product of the number of turns and the effective area, NS, of the new MMP is $7.9 \times 10^{-4} \text{ m}^2$, which is about 8 times as large as that of the old MMP. The new MMP has ten coils located with a distance of 10 mm between adjacent coils. No signal is available for the 7th coil from the inside due to disconnection. Figure 3 shows a plane view and a cross-section

view of TOKASTAR-2. The radius of the vacuum vessel is 0.3 m and its height is 0.6 m. The MMP is located in one of the four large ports on the side wall of the vacuum vessel, which is at a toroidal angle of 90 degrees as shown in Fig. 3 (a). The MMP is inserted through a gauge port on the port flange. The range of $65 \text{ mm} \leq R \leq 265 \text{ mm}$ can be measured by MMP by moving the MMP radially shot by shot.

The radial plasma position is defined by the plasma major radius R_p that is the major radius of the center of plasma cross section. In this study, we used the radial profile of the Z-component of the poloidal field, B_z , measured by the MMP inserted into plasma, to determine R_p . The magnetic field is generated by the coil currents, the plasma current and the eddy current in the vacuum vessel. The Z-component of the field generated by the plasma current B_z^{pl} was obtained by subtracting the Z-component of the vacuum magnetic field B_z^{vac} from the field measured with the plasma current, B_z^{tot} . The B_z^{vac} was obtained by turning off the microwave injection to suppress the plasma generation but with the same charging voltage of the capacitors for the OH coil power supply and the PVF coil power supply. Then the coil current waveforms were nearly identical for the shots with and without the plasma current. It is assumed that the field measured in a shot without the plasma current is equal to the field generated by the coil current and the eddy current in a shot with the plasma current.

The plasma major radius R_p was determined by fitting the measured B_z^{pl} with the calculated one. The calculated value of B_z^{pl} is obtained analytically by assuming concentric circular flux surfaces on the poloidal plane [7]. Note that in this analysis it is assumed that the plasma center is located on the midplane and the plasma edge is attached on the inner or outer limiter ($R = 75 \text{ mm}$ or $R = 172 \text{ mm}$). Then the radial distribution of the B_z^{pl} is determined solely by R_p , for a given current density profile. In this study, the innermost MMP channel was located at $R = 120 \text{ mm}$, namely nearly in the middle of inner and outer walls, so as not to have a large influence on the tokamak plasma [7]. Then the innermost channel was located around the plasma center. Figure 4 shows an example of determination of R_p . The measured values are well fitted by a calculated curve for R_p of 115 mm, shown by the central vertical line. Note that although B_z^{pl} plotted here is not zero at the plasma center or the magnetic axis, the Z-component of the total field should be zero there since B_z^{pl} is canceled by the vacuum vertical field. In this analysis, the plasma current density profile is assumed to be proportional to $(1 - (r/a)^2)^{0.1}$ namely to have a nearly flat profile, where r and a denote the minor radius and the plasma minor radius, respectively. This is the case for typical tokamak plasmas in TOKASTAR-2. The assumption of the circular cross section with concentric flux surfaces was made considering results of a predictive MHD equilibrium analysis [3]. It seems to be verified by the fact that the measured values

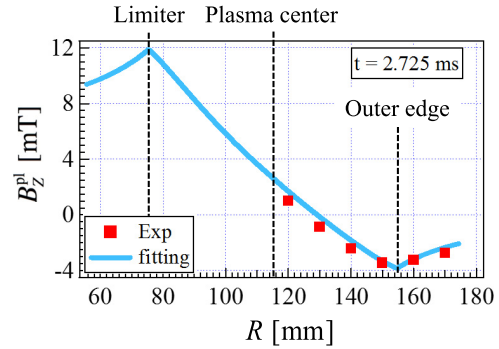


Fig. 4 An example of determination of the radial plasma position using the data obtained with the new MMP after modification of PVF coils and installation of the poloidal limiter. The red squares denote the measured Z-component of the poloidal field and the light blue line denotes the calculated one. The major radii of the inner limiter surface, the plasma center and the outer edge of the plasma column are shown by vertical dotted lines.

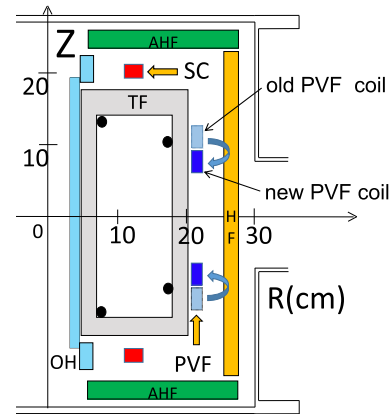


Fig. 5 Cross-section view of the device showing modification of the PVF coil positions and installation of new SC coils. The old and new PVF coil positions are shown by light blue and deep blue, respectively, while the SC coils are shown by red.

are relatively well fitted by the assumed function as shown in Fig. 4. Images of high speed camera also show that the cross section is not highly elongated. Furthermore, recent analysis using external magnetic probes confirms nearly circular cross sections [10].

2.3 Improvement of the decay index

To improve the decay index profile and obtain stable tokamak plasma in the outer region, modification was made on the PVF coils in parallel with installation of the poloidal limiter in April 2016. The vertical position of the PVF coils was changed to $Z = \pm 80 \text{ mm}$ from $Z = \pm 108 \text{ mm}$, as shown in Fig. 5, to increase the vertical field in the outer region and improve decay index there. The new vertical position was determined so as to keep a space,

with a gap of 5 mm, for the in-vessel mirror that is located between the upper and lower PVF coils [8].

The measured B_Z^{vac} and the fitted curve are shown by closed blue circles and a blue line respectively in Fig. 6 (a) for the original PVF coil positions. The data was taken at $t = 2.8$ ms at which the plasma current reaches its peak typically. The charging voltage of the capacitor for the OH coil circuit was 2.0 kV. The OH coil current was 1.70 kA and PVF coil current was 0.18 kA.

The original PVF coil set, a so-called Helmholtz coil, generates a nearly flat vertical field between the inner and outer limiters, which satisfies the stability condition $0 < n < 1.5$ in a wide range of $75 \text{ mm} \leq R \leq 160 \text{ mm}$. A large eddy current is, however, generated in the TOKASTAR-2 vacuum vessel by the loop voltage induced by the OH coil current [3]. The vertical field generated by the eddy current is nearly uniform and in the opposite direction to the vertical field generated by the PVF coil current and cancels more than half of it. As a result, the vertical field becomes zero near the surface of the outer limiter ($R = 172 \text{ mm}$) as shown by a blue curve in Fig. 6 (a) and the range with $n < 1.5$ is restricted to $R < 120 \text{ mm}$ as shown by a blue curve in Fig. 6 (b). This may restrict the possible operation range of the plasma position to the inner region. In contrast, the helical field is stronger in the outer region as shown in Fig. 7 and hence experiment with tokamak plasma in the outer region is preferable to see the effect

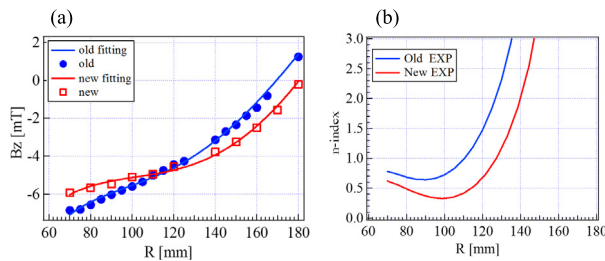


Fig. 6 Comparison between the radial profiles of (a) B_Z^{vac} and (b) the decay index before (a blue solid line) and after (a red solid line) modification of the PVF coil positions.

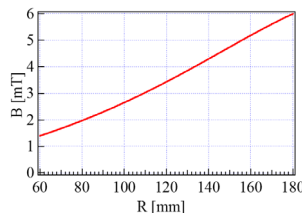


Fig. 7 Radial distribution of the magnitude of the helical field at $Z = 0$ and at the toroidal angle of the MMP ($\phi = 90^\circ$) generated by HF, AHF and VF coils. The field is calculated with typical coil currents used in the experiment; 2.5 kAturns, 2.9 kAturns and 150 Aturns for the HF coil, the AHF coil and the VF coil, respectively.

of helical field application.

The radial profiles of B_Z^{vac} and the decay index after modification of the PVF coil are shown by red curves in Fig. 6. The PVF coil current at $t = 2.8$ ms was adjusted to 0.13 kA so that the vertical field in the inner region ($R = 110 \text{ mm}$) is unchanged compared to the value before the modification. The stable region with $n < 1.5$ was expanded from $R < 120 \text{ mm}$ to $R < 135 \text{ mm}$. Improvement of decay index was thus confirmed.

3. Results of Plasma Experiment

We performed tokamak operation with the modified PVF coils. The MMP was inserted into the plasma to measure the radial plasma position. The PVF coil current was scanned shot by shot for a fixed charging voltage (2.0 kV) of the capacitor for the OH coil circuit. With this scan we can find the optimum charging voltage (current) for the PVF coils that maximizes the peak value and/or the duration of the plasma current [11]. The plasma current and the plasma major radius R_p at $t = 2.7$ ms are shown as functions of the vertical field at the same time in Fig. 8. The radial plasma position moved outward with decrease in the absolute value of the vertical field, but it stayed at nearly the same position for the sufficiently weak vertical field, both before and after the modification. The largest plasma major radius was $R_p = 123 \text{ mm}$ after the modification while it was $R_p = 112 - 120 \text{ mm}$ before the modification. Namely the outermost position of the plasma center was shifted by about 7 mm outward. In addition, the

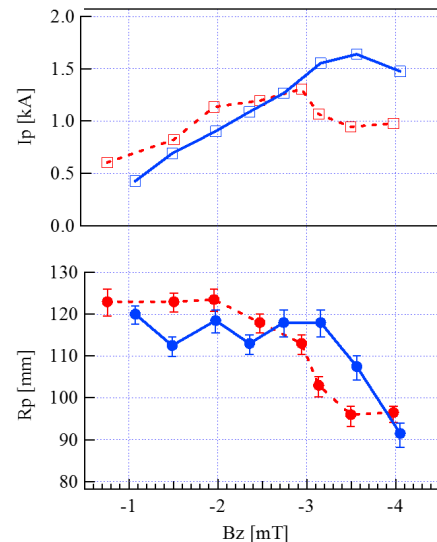


Fig. 8 (upper) The plasma current and (lower) the plasma major radius as functions of the vertical field at $R = 0.12 \text{ m}$. Blue solid lines denote the values before modification of the PVF coil positions while red broken lines denote the values after the modification. The values of plasma current, the plasma major radius and the vertical field are evaluated at $t = 2.7$ ms.

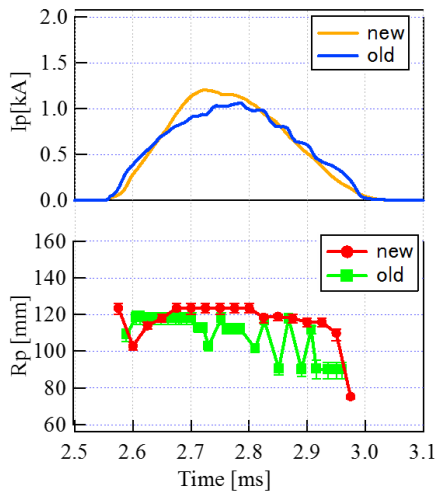


Fig. 9 Time evolution of (upper) the plasma current and (lower) the plasma major radius in the two shots before the modification (denoted by “old”) and after the modification (denoted by “new”) with the vertical field of -2 mT shown in Fig. 8.

plasma current was larger in the weak vertical field range $|B_z| < 2.5$ mT after the modification than before the modification, as shown in the upper panel of Fig. 8. On the other hand, the plasma current was smaller after the modification in the strong vertical field range. One possible reason is the larger interaction between the plasma and the inner wall after the insertion of the poloidal limiter.

Figure 9 shows time evolution of the plasma current and R_p for two shots with $|B_z| = 2$ mT shown in Fig. 8. Rapid oscillation in the plasma current and R_p were observed in the shot before the modification, while they were not observed in the shot after the modification.

The results shown in Figs. 8 and 9 indicate that tokamak plasma was stably generated in the outer position after the modification than before. This result seems to be caused by improvement in the decay index, though the radial shift in the plasma position (7 mm) was smaller than that in the decay index curve (15 mm). The outer limit of the radial plasma position, $R = 123$ mm, is almost in the middle ($R = 124$ mm) of the inner wall ($R = 75$ mm) and the outer wall ($R = 172$ mm). The wall limits the plasma is switched from the inner wall to the outer wall when R_p exceeds the middle of the inner and outer walls, 124 mm. It is not understood yet whether touching the outer wall has any effects on evolution of the radial plasma position or not.

Initial results of application of helical field on tokamak plasma after modification of the PVF coils is reported in [10]. Figure 7 of [10] shows the peak plasma current I_p^{peak} as a function of the vertical field. In these discharges, MMP was not inserted into the plasma and hence the plasma current was higher than those shown in Figs. 8

and 9. For the vertical field weaker than the optimum value, where I_p^{peak} becomes maximum, no clear effects of the helical field on I_p^{peak} is recognized, as was seen before modification of the PVF coil as shown in Fig. 3 in [8]. In contrast, it can be seen that I_p^{peak} was higher with the helical field than without the helical field for strong vertical field, which was not observed before modification of the PVF coil. Note that this is due mainly to degradation of plasma current without the helical field for strong vertical field after modification of the PVF coil, which seems to be caused by reduction of decay index in the inner region as shown in Fig. 6 (b). Detailed comparison on the effect of helical field before and after modification of the PVF coil, including the analysis of time evolution of the plasma radial position, will be studied and reported in future.

4. Conclusion

The decay index has been improved and the range of the stable radial plasma position has been extended to the outer region owing to modification of the PVF coil positions in TOKASTAR-2. The outermost position of the plasma center was shifted by about 7 mm outward, which was smaller than outward shift in the decay index curve (15 mm). The application of helical field resulted in increase in the peak plasma current for strong vertical field while no clear effects in the peak plasma current for the optimum and weak vertical field.

Acknowledgments

This work was performed with the support and under the auspices of the NIFS Collaboration Research program (NIFS14KOAP027) including the NIFS Joint Use Program of Measurement Instruments.

- [1] T. Oishi, K. Yamazaki, K. Okano *et al.*, J. Plasma Fusion Res. SERIES **9**, 69 (2010).
- [2] M. Hasegawa, K. Yamazaki, H. Arimoto *et al.*, Plasma Fusion Res. **7**, 2402116 (2012).
- [3] R. Nishimura, H. Arimoto, T. Fujita *et al.*, Plasma Fusion Res. **9**, 3402059 (2014).
- [4] H. Ikezi, K.F. Shwarzenegger and C. Ludescher, Phys. Fluids **22**, 2009 (1979).
- [5] W VII-A TEAM, Nucl. Fusion **20**, 1093 (1980).
- [6] M.D. Pandya, M.C. ArchMiller, M.R. Cianciosa *et al.*, Phys. Plasmas **22**, 110702 (2015).
- [7] T. Ueda, H. Arimoto, T. Fujita *et al.*, Plasma Fusion Res. **10**, 3402065 (2015).
- [8] T. Sakito, H. Arimoto, T. Fujita *et al.*, Plasma Fusion Res. **11**, 2402074 (2016).
- [9] V.S. Mukhovatov and V.D. Shofranov, Nucl. Fusion **11**, 605 (1971).
- [10] K. Yasuda, H. Arimoto, T. Fujita *et al.*, Plasma Fusion Res. **13**, 3402072 (2018).
- [11] T. Sakito, H. Arimoto, T. Fujita *et al.*, Plasma Fusion Res. **10**, 3402033 (2015).